Supporting information

Appendix S1: Release effort of captive bred houbaras from 1998 to 2018 in the ECWP intervention area

Figure A1-1: Cumulative release effort per month from 1998 to 2018.

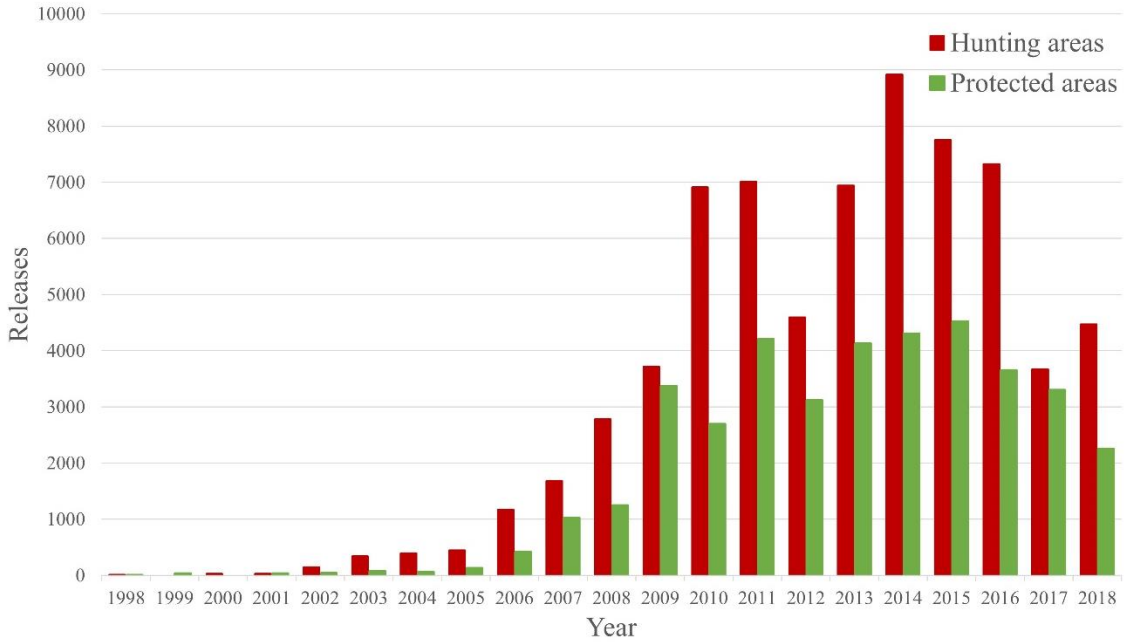

Figure A1-2: Release effort per year from 1998 to 2018.

Up to 2016, hunting areas and protected areas covered respectively 64% and 36% of the ECWP intervention area. In 2017, a new 5 500 km² protected area was created in the east of the region, along

Algerian boarder, raising the surface of the protected areas up to 47 % of the ECWP intervention area (Fig. 1).

Appendix S2: Counting effort

Since 2000, ECWP counting effort in the ECWP intervention area has changed. Initially (2000-2001) a general survey was organized with the aim of benchmarking the houbara abundance on the area. From 2002 to 2006, the counts were concentrated on 2 areas (one hunted and one protected), with 4 counts per year. From 2007, it was decided to make only one fall count per area every year. Progressively the number of areas was increased to reach the current pattern (2018), in order to have a better representativeness each year. In each counting session and at each counting point, birds were counted during 20 minutes within a 3 km radius by two observers using binoculars. Counting occurred within three hours after sunrise and 2 hours before sunset. Observers started their observation at opposite bearing and turned in same directions. They shared their sightings during their respective 360° circular observation to avoid recording duplicates.

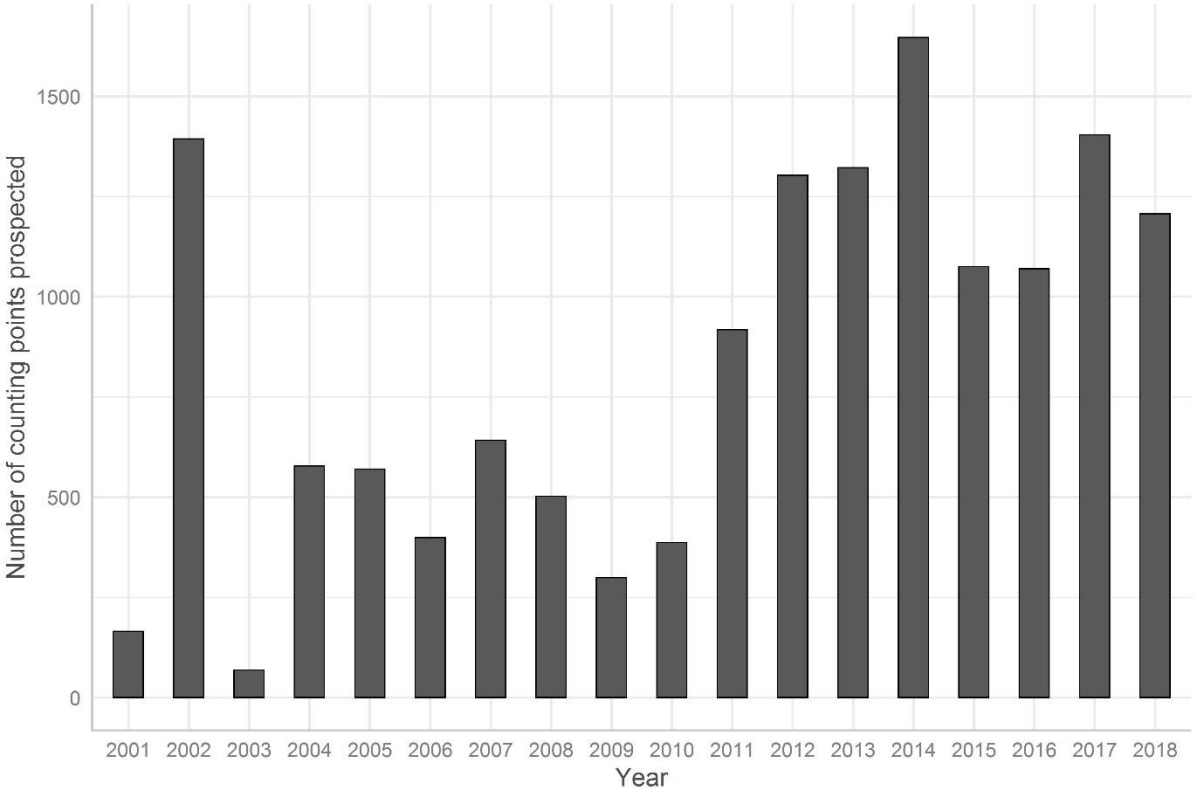

Figure A2-1: Change in houbara counting effort within the ECWP intervention area in Morocco between 2001 and 2018.

After the 20 minutes of observation, the observers visited locations where individuals or groups were sighted at first and recorded the exact coordinates using a GPS. This allowed the measurement of the

accurate distance from the counting point to each bird (or group of birds) observed. In addition, at each counting session, the following information were recorded: elevation, dominant plant species, observer's names, coordinates of anthropogenic elements (transport infrastructure, dam, hut, house, fixed enclosure), wildlife (ungulates, canids, felines, raptors) and the number of livestock animals present around the counting point. Teams of observers were often modified to minimize observer bias. A counting session was cancelled if the point was not accessible or if the observation conditions were not optimal at 360° because of strong wind, heavy rain or heat waves. A minimum number of observations is required for an accurate density estimate. Below this quota, counting is repeated on the same area until the desired number of observations is reached. Across the area, 843 counting points were created in 10 zones.

Appendix S3: Spatializing the abundances using density surface modelling

Density surface modelling (hereafter: "dsm") provides an approach to spatialize abundance estimates from remote sampling data (Miller *et al.*, 2013). A dsm uses observations of individuals or groups of individuals, assigns them to segments and adjusts counts based on detectability using the detection function model. A generalized additive model (GAM) is then used to model these adjusted counts according to a formula involving or not covariates. Using the "dsm" package version 2.3.0 (Miller *et al*., 2020), we opted for modelling the estimation of houbara abundance as a function of space only, using a Tweedie response distribution. Tweedie's response provides good flexibility to the model (Miller *et al*., 2013). We generated predictions about how the estimated abundance of houbara was distributed in space. Results were projected in a 5-arcminute grid that excluded habitat unsuitable for the houbara: (1) mountainous areas with slopes greater than 5%, previous work on individually monitored birds (1,284,427 locations recorded via GPS satellite tracking and GSM-GPS out of 512 individuals between 2005 and 2017, unpublished data) showed that 99% of houbara tracking locations occur in areas with slopes of less than 5%; (2) urban areas with a buffer zone of 10 km around cities (Fig. A3-1). After exclusion of unsuitable areas, the total area of predicted abundances represented 38,268 km² (76% of the 50,170 km² of the ECWP intervention area).

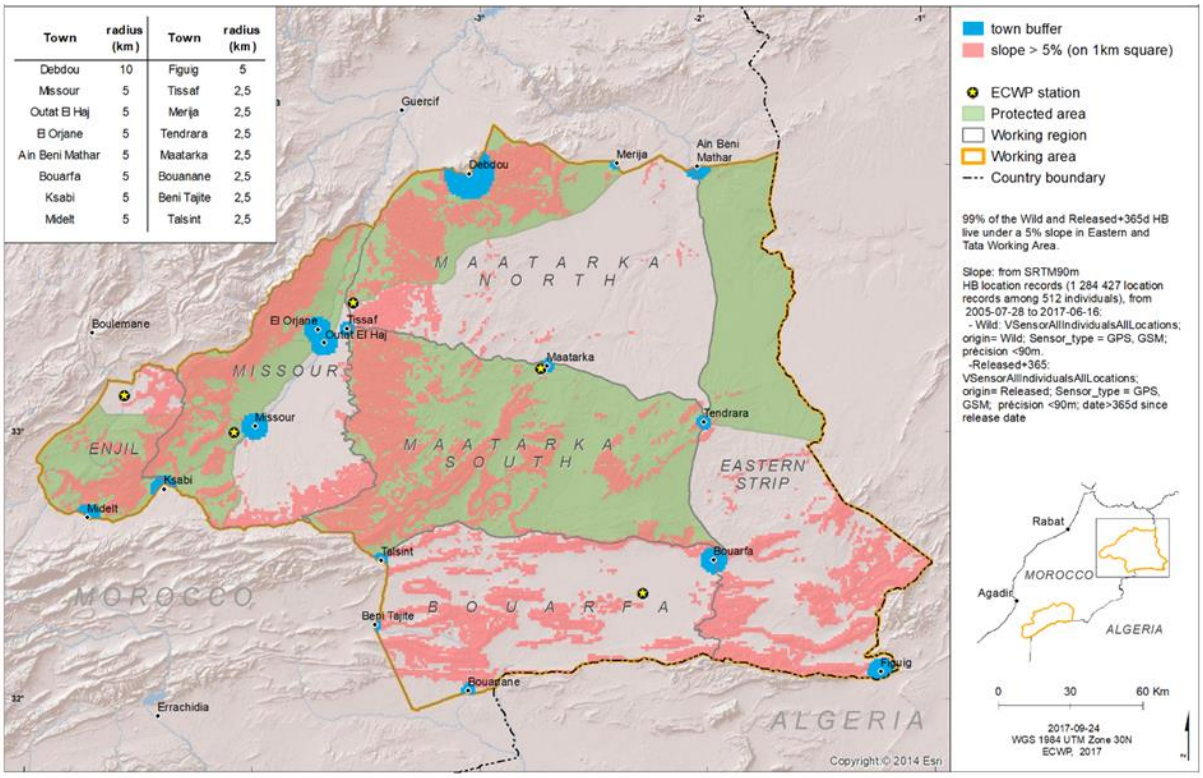

Figure A3-1: Mask of the unsuitable areas for houbara in the ECWP intervention area in Morocco. Areas excluded from the dsm are highlighted in blue (urban areas) and pink (areas with slopes >5%)

To examine whether houbara local abundances varied consistently over time, we produced Hovmöller diagrams (Hovmöller, 1949) illustrating the changes in houbara abundances according to latitude and longitude (by degree) and time (by year). The Hovmöller diagrams average all the values of a single column of longitude or a line of latitude. In our case, we averaged the abundance estimates per pixel by latitude and longitude bands for each year. We excluded the year 2010 because of its high uncertainty associated with the dsm abundance estimates (see results).

Appendix S4: Releases effort variable

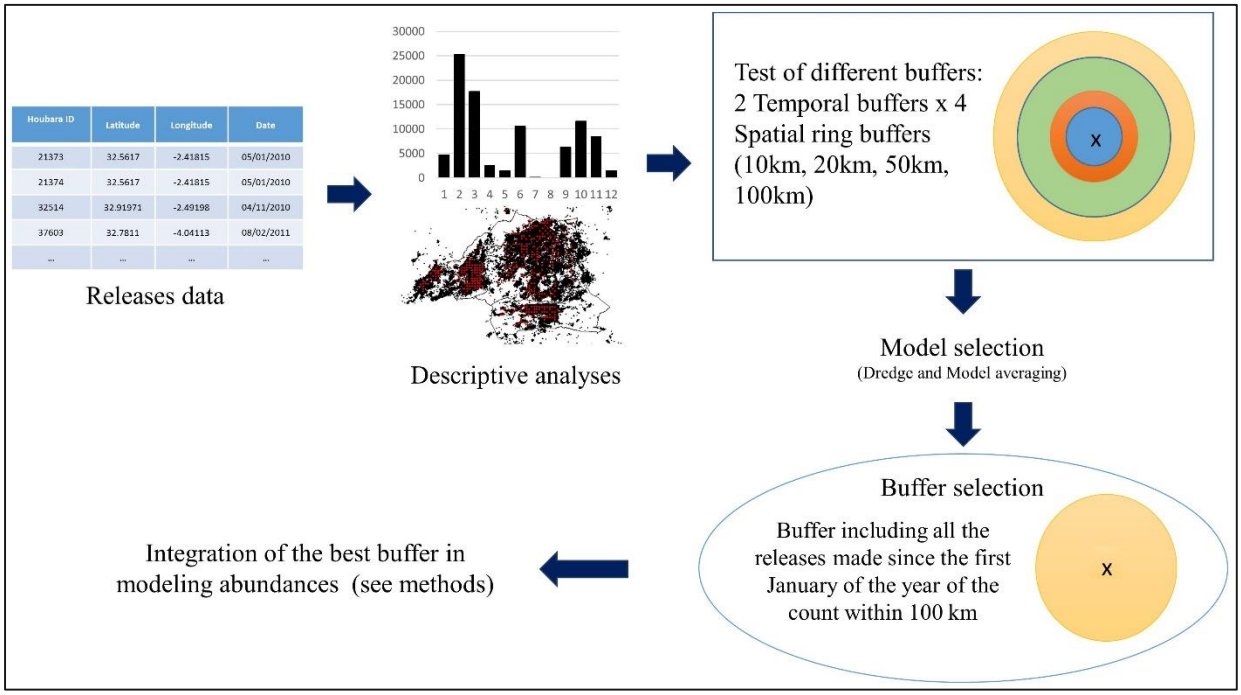

Figure A4-1: Summary of the analyses used to extract the release effort variable

To include the release effort variable in the model it was first necessary to test the relationship between the estimated abundance at a counting point and the amount of releases made around it. However, knowing that houbara release effort varied between points and individuals move with time from the release location, the abundance at one point might be influenced not only by the amount of birds released on this point, but also on the neighboring points. Then, around the counting point, we created different spatial buffers of radius r_i which each included different numbers of individuals released depending on the size of r_i. In addition, as several releases might have occurred in the same area over the year and because dispersal is associated with time, we considered temporal buffers n_i corresponding to different numbers of days prior to the counting date.

Descriptive analyses

To select the most relevant buffer values (r and n) we first analyzed dispersal of captive bred released houbara (N= 347,034) tracked (GPS PTT and GPS GSM) between 2010 and 2017. The movement, i.e. the distance travelled by an individual after n_i days, was calculated using the net linear distance between the release site and the location of the individual at day n_j.

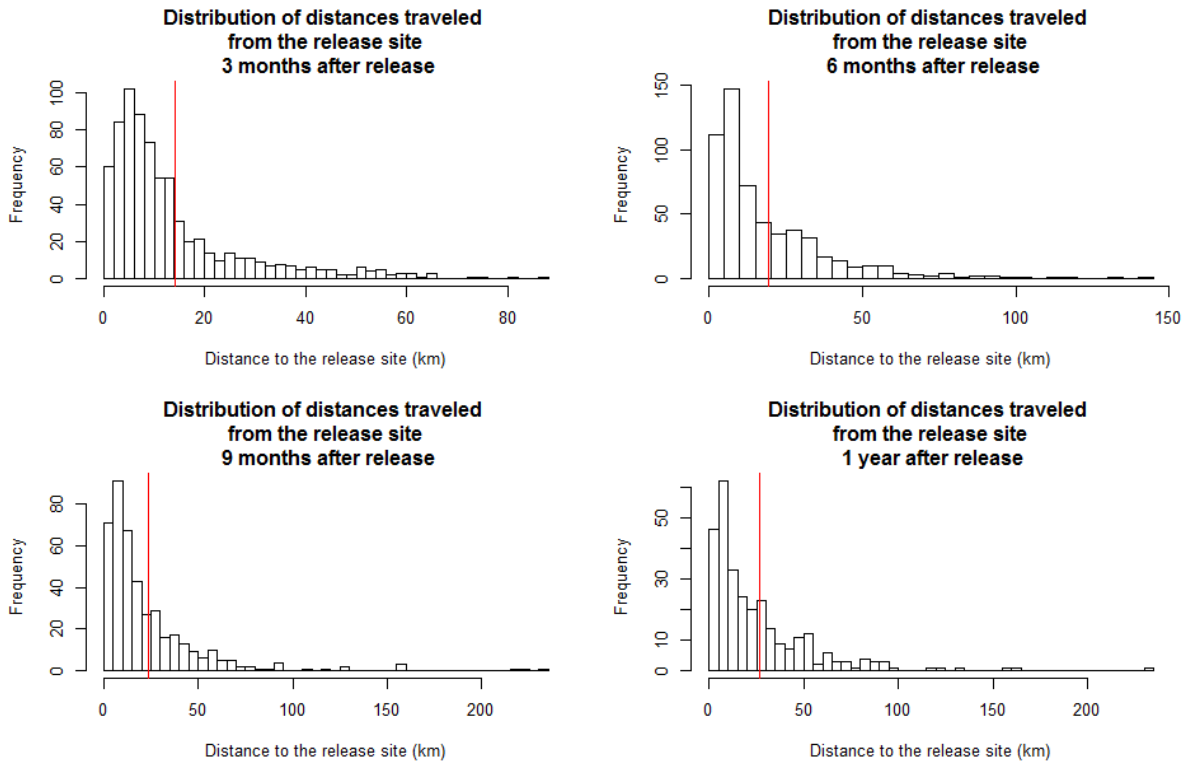

Figure A4-2: Distribution of distance traveled from the release site by houbara (a) 3 months after release; (b) 6 months after release; (c) 9 months after release; (d) one year after release. Red bar represents the mean distance traveled.

Temporal buffers, n_i

For the temporal buffers we selected two approaches considering the release and the counting strategies. For each point, the first temporal buffer chosen corresponded to one year before the date of the count (hereafter: BY) and the second corresponds to the period between the first January of the count year and the date of the count (hereafter: BJ).

Spatial buffers, r_i

To study the movement of houbara, we looked at the distances travelled every three months since the date of release (Fig. A4-1). Looking at the movement data, we found that the average distance travelled by a captive-bred houbara from its release sites was 28 km, with the maximum distance observed being 235 km one year after release. We have selected four spatial buffers with 10km, 20km, 50km and 100km distance around the counting point. Thus, the 100 km buffer included all releases between 50 km and 100 km from the counting point. The 50 km buffer included all individuals released between 20 km and 50 km from the counting point. The 20 km buffer included all individuals released between 10 km and

20 km from the counting point. The 10 km buffer included all individuals released between the counting point and 10 km around the counting point. We then calculated a total of 4x2 buffers, combining the temporal and spatial buffers selected.

Model selection

In order to test which buffer had the highest effect on abundance we used a zero-truncated model because of the large number of zeros and the over dispersion of the estimated abundances data. Zero-truncated models consisted of two parts: data were first considered as zero vs non-zero. A binomial model was used to model the probability that a zero was observed; in a second step the non-zero observations were modelled with a truncated Poisson model or a truncated negative binomial model. In both parts the use of covariates was possible. The model: Abundance ~ BJ10 + BJ20 + BJ50 + BJ100 + BY10 + BY20 + BY50 + BY100 was tested with different distribution (Poisson, Negative Binomial). different random effect (Year, Latitude) and different formulas in the binomial part of the model (simple model or with covariates); i.e. 17 models tested.

Table A4-1: 15 of the best models out of the 17 tested, ranked by AIC criteria

	Model	**Y**	**Covariate**	**Zero-inflated covariate**	**Distribution**	**Delta AIC**
1	M15	Nc	log(Buffers)+(1|Year)+(1|LAT)	log(Buffers)+(1|Year)+(1|LAT)	negative binomial	0
2	M11	Nc	log(Buffers)+(1|LAT)	log(Buffers)+(1|LAT)	negative binomial	190.8
3	M13	Nc	log(Buffers)+(1|Year)+(1|LAT)	1	negative binomial	863.8
4	M9	Nc	log(Buffers)+(1|LAT)	1	negative binomial	1031.4
5	M16	Nc	log(Buffers)+(1|Year)+(1|LAT)	log(Buffers)+(1|Year)+(1|LAT)	poisson	1469.4
6	M7	Nc	log(Buffers)+(1|Year)	log(Buffers)+(1|Year)	negative binomial	1610.7
7	M5	Nc	log(Buffers)+(1|Year)	1	negative binomial	1860.9
8	M3	Nc	log(Buffers)	log(Buffers)	negative binomial	1907.9
9	M1	Nc	log(Buffers)	1	negative binomial	2006.7
10	M0	Nc	1	1	negative binomial	2106.7
11	M14	Nc	log(Buffers)+(1|Year)+(1|LAT)	1	poisson	2333.1
12	M12	Nc	log(Buffers)+(1|LAT)	log(Buffers)+(1|LAT)	poisson	2391.8

We studied the weight of the covariates of the best model, the model M15. The classical approach (dredge), which consisted in testing all possible combinations, was not used due to the type of model used and the data set. We therefore tested several sub-models from M15 by including conditions: if a buffer with radius X was included in the sub-model, buffers with radii smaller than X were included in the sub-model (example: sub-model including buffer BY50 necessarily includes buffers BY10 and BY20). At the end, 600 models were tested, using all possible combinations of buffers (in the conditional part of the model and in the *ziformula* part). The top 30 models were selected, based on the AIC criteria, and then model averaging was performed on these models.

Buffer selection

We looked at the relative importance of the different parameters, using the model weights. The Akaike weights for each model containing the parameter of interest were summed (Table A4-2). All the BJ were more present in the 30 best models, and their importance weights were higher than those of the BY.

Table A4-2: Relative importance of the parameters using the Akaike weight

Variable	**Sum of weights**	**N containing model**
BJ100	***1.00***	***29***
BJ10	***1.00***	***29***
BJ20	***1.00***	***29***
BJ50	***1.00***	***29***
BY10	0.95	25
BY20	0.86	20
BY50	0.79	15
BY100	0.78	12

We then looked at the model-averaged coefficients (Full average. Table A4-3). The “full” average assumes that a variable is included in every model, but in some models the corresponding coefficient (and its respective variance) is set to zero. BJ100 (ring buffer) was the only variable that had a significant effect on abundance.

Table A4-3: Model-average coefficients (Full average) for the significant parameters

	Estimate	St. Error	Adjusted SE	Z value	Pr(>|Z|)	
Conditional model						
Intercept	2.078	0.719	0.719	2.88	0.003	***
BJ100	0.229	0.084	0.084	2.72	0.006	**
Ziformula						
Intercept	-3.330	1.062	1.062	3.13	0.001	**
BY100	-0.046	0.186	0.186	1.92	0.054	.

Best buffer

After all the analyses we selected the buffer BJ100, as disk buffer (i.e. a buffer including all releases within a 100 km radius of the counting point) for the releases covariate. Thus the releases covariate constructed corresponded to the number of houbaras released in a buffer of 100 km around the counting point, including all the releases made since the first January of the year of the count.

Appendix S5: Zero Inflated models

Zero-inflated models are used to model count data with an excess of zero and over-dispersed (Zuur *et al*., 2009). A zero, (i.e. an absence) can be the result of different processes: the bird is not there because the habitat is not suitable, the observer did not see the animal because there was something on the counting point that was hiding it, the habitat is suitable but there is no bird there.

Zero-inflated models consider that the response variable contains more zeros than expected. Zero-inflated models model the zeros as if they could come from two distinct processes: a binomial process or a counting process. First, a binomial GLM is used to model the probability of having a zero. The second part, the counting process, is modeled by a Poisson or negative binomial GLM. These zeros are considered "true zeros", counts where no individual is observed; "false zeros" are modeled by the binomial model (they are generated by structural, protocol design or observer errors; Brooks *et al.*, 2017).

The fitted model is thus divided into two parts: a conditional model, which corresponds to the abundance/count modelling, and a zero inflation part, which corresponds to the absence.

Appendix S6: Houbara abundance estimation per year, from 2010 to 2018

Table A6: Houbara abundance estimation in the ECWP intervention area of Morocco using the distance sampling method

Label	Estimate	se	cv	lcl	ucl	df
2010	32,401	4,562	0.141	24,608	42,662	641
2011	22,821	2,421	0.106	18,544	28,084	1,481
2012	12,307	1,114	0.090	10,310	14,691	2,281
2013	10,409	974	0.094	8,667	12,500	2,411
2014	10,506	994	0.095	8,731	12,642	3,161
2015	19,857	1,986	0.100	16,329	24,147	2,037
2016	16,903	1,598	0.095	14,049	20,338	2,218
2017	13,857	1,645	0.119	10,988	17,475	2,317
2018	13,207	1,590	0.120	10,438	16,710	2,283

The abundances per year were estimated by the detection function and the density surface modelling. There is not a clear trend in abundances (Fig. 1). The average abundance over the nine years is 16,918 individuals [13,629 – 21,027] with the highest relative abundance within the time of the study occurring in 2010 and the lowest occurring in 2013 (Table A6).

Appendix S7: Model selection

We developed different models to study the temporal and spatial variation in houbara abundances using *Nc* (the local abundance during a counting session corrected by the probability of detection) as the response variable. We used zero-inflated models (see details in Supporting Information Appendix S5) to account for over-dispersion of these data and excess of zeros. We tested several zero-inflated models with different distributions (Poisson or negative binomial) and various covariate combinations in the argument to model extra zeros: Hunting, Year and Nrel (these models are numbered 1 through 8, see Table A7-1). We added some interactions on those models: (i) between the precipitation anomaly and the mean precipitation at the focal pixel (Panom:Prec); (ii) between temperature anomaly and the mean temperature at the focal pixel (Tanom:Temp); and (iii) between the management of the zone and the number of releases (Hunting:Nrel). We used AIC to select the most parsimonious model between the 48 models tested (see Table A7-2). Zero-inflated models were implemented with the "glmmTMB" package version 0.2.3 (Magnusson et al., 2017) of R.

Table A7-1: The eight initial models without interaction. The conditional part of each of the eight models includes all the main fixed-effect covariates (Year, Town, Road, Nrel, Hunting, Livestock, Habitat, Tanom, Panom, Temp and Prec).

Model	Zero-inflation part	Distribution
Mod1	~ 1	Poisson
Mod2	~ 1	Negative binomial
Mod3	~ Hunting	Poisson
Mod4	~ Hunting	Negative binomial
Mod5	~ Year	Poisson
Mod6	~ Year	Negative binomial
Mod7	~ Nrel	Poisson
Mod8	~ Nrel	Negative binomial

Table A7-2: AIC table comparison between tested models. Delta AIC refers to the relative difference of AIC score between the best model (which has a Delta AIC of zero) and the others models.

Model	Interaction	Delta AIC	df
Mod6a	Panom:Prec	0,0	31
Mod6		0,2	30
Mod6d	Hunting:Nrel	0,7	31
Mod6c	Panom:Prec + Tanom:Temp	2,0	32
Mod6b	Tanom:Temp	2.1	31
Mod6e	Hunting:Nrel + Panom:Prec + Tanom:Temp	2.4	33
Mod8a	Panom:Prec	156.1	24
Mod8		156.4	23
Mod8d	Hunting:Nrel	156.7	24
Mod8c	Panom:Prec + Tanom:Temp	158.1	25

Mod8b	Tanom:Temp	158.2	24
Mod8e	Hunting:Nrel + Panom:Prec + Tanom:Temp	158.5	26
Mod4a	Panom:Prec	187.3	24
Mod4		187.6	23
Mod4d	Hunting:Nrel	187.9	24
Mod4c	Panom:Prec + Tanom:Temp	189.3	25
Mod4b	Tanom:Temp	189.4	24
Mod4e	Hunting:Nrel + Panom:Prec + Tanom:Temp	189.7	26
Mod2a	Panom:Prec	193.5	23
Mod2		193.8	22
Mod2d	Hunting:Nrel	194.1	23
Mod2c	Panom:Prec + Tanom:Temp	195.5	24
Mod2b	Tanom:Temp	195.6	23
Mod2e	Hunting:Nrel + Panom:Prec + Tanom:Temp	195.9	25
Mod5e	Hunting:Nrel + Panom:Prec + Tanom:Temp	134408.3	32
Mod5d	Hunting:Nrel	134429.4	30
Mod5c	Panom:Prec + Tanom:Temp	134443.3	31
Mod5a	Panom:Prec	134447.6	30
Mod5		134466.4	29
Mod5b	Tanom:Temp	134466.7	30
Mod7e	Hunting:Nrel + Panom:Prec + Tanom:Temp	134565.4	25
Mod7d	Hunting:Nrel	134586.5	23
Mod3e	Hunting:Nrel + Panom:Prec + Tanom:Temp	134596.6	25
Mod7c	Panom:Prec + Tanom:Temp	134600.4	24
Mod1e	Hunting:Nrel + Panom:Prec + Tanom:Temp	134602.4	24
Mod7a	Panom:Prec	134604.7	23
Mod3d	Hunting:Nrel	134617.8	23
Mod7		134623.4	22
Mod1d	Hunting:Nrel	134623.6	22
Mod7b	Tanom:Temp	134623.8	23
Mod3c	Panom:Prec + Tanom:Temp	134631.7	24
Mod3a	Panom:Prec	134636.0	23
Mod1c	Panom:Prec + Tanom:Temp	134637.5	23
Mod1a	Panom:Prec	134641.8	22
Mod3		134654.7	22
Mod3b	Tanom:Temp	134655.0	23
Mod1		134660.5	21
Mod1b	Tanom:Temp	134660.9	22

Appendix S8: Factors related to abundance

Table A8: Summary of the best generalized linear mixed model regressing corrected abundance of houbara against spatial and temporal variables; with a negative binomial distribution and the Year as zero-inflation parameter. CI is 95% confidence interval.

	Estimate	**Lower CI**	**Upper CI**	**Standard Error**	**z value**	**p-value**
	Conditional part					
(Intercept)	4.174	4.036	4.312	0.07	59.38	$< 10^{-3}$
Year2011	-0.061	-0.224	0.102	0.083	-0.74	0.461
Year2012	-0.491	-0.639	-0.344	0.075	-6.52	$< 10^{-3}$
Year2013	-0.665	-0.813	-0.518	0.075	-8.84	$< 10^{-3}$
Year2014	-0.47	-0.64	-0.3	0.087	-5.41	$< 10^{-3}$
Year2015	-0.135	-0.286	0.016	0.077	-1.75	0.08
Year2016	-0.214	-0.408	-0.02	0.099	-2.17	0.03
Year2017	-0.097	-0.306	0.111	0.106	-0.92	0.36
Year2018	-0.325	-0.564	-0.085	0.122	-2.66	0.008
Town	0.023	-0.014	0.059	0.019	1.21	0.225
Road	-0.009	-0.045	0.028	0.019	-0.47	0.642
N_{rel}	0.08	0.026	0.133	0.027	2.93	0.003
Hunting	0.436	0.358	0.514	0.04	10.96	$< 10^{-3}$
Livestock	0.041	0.022	0.061	0.01	4.14	$< 10^{-3}$
Hab_{mosaic}	-1.928	-3.69	-0.165	0.899	-2.14	0.032
Hab_{vege}	-0.05	-0.135	0.036	0.044	-1.13	0.257
T_{anom}	0.029	-0.036	0.093	0.033	0.87	0.384
P_{anom}	0	-0.05	0.049	0.025	-0.01	0.991
Precip	-0.037	-0.085	0.01	0.024	-1.53	0.125
Temp	-0.129	-0.172	-0.086	0.022	-5.86	$< 10^{-3}$
	Zero-inflation part					
(Intercept)	0.185	0.001	0.369	0.094	1.972	0.049
Year2011	0.359	0.136	0.582	0.114	3.152	0.002
Year2012	0.575	0.36	0.789	0.11	5.241	0
Year2013	0.769	0.551	0.986	0.111	6.932	0
Year2014	1.154	0.936	1.372	0.111	10.375	< 2e-16
Year2015	0.638	0.415	0.86	0.114	5.612	0
Year2016	0.677	0.454	0.901	0.114	5.945	0
Year2017	1.192	0.962	1.422	0.117	10.148	< 2e-16
Year2018	1.062	0.772	1.353	0.148	7.17	0

Appendix S9: Uncertainty of density surface modelling (dsm)

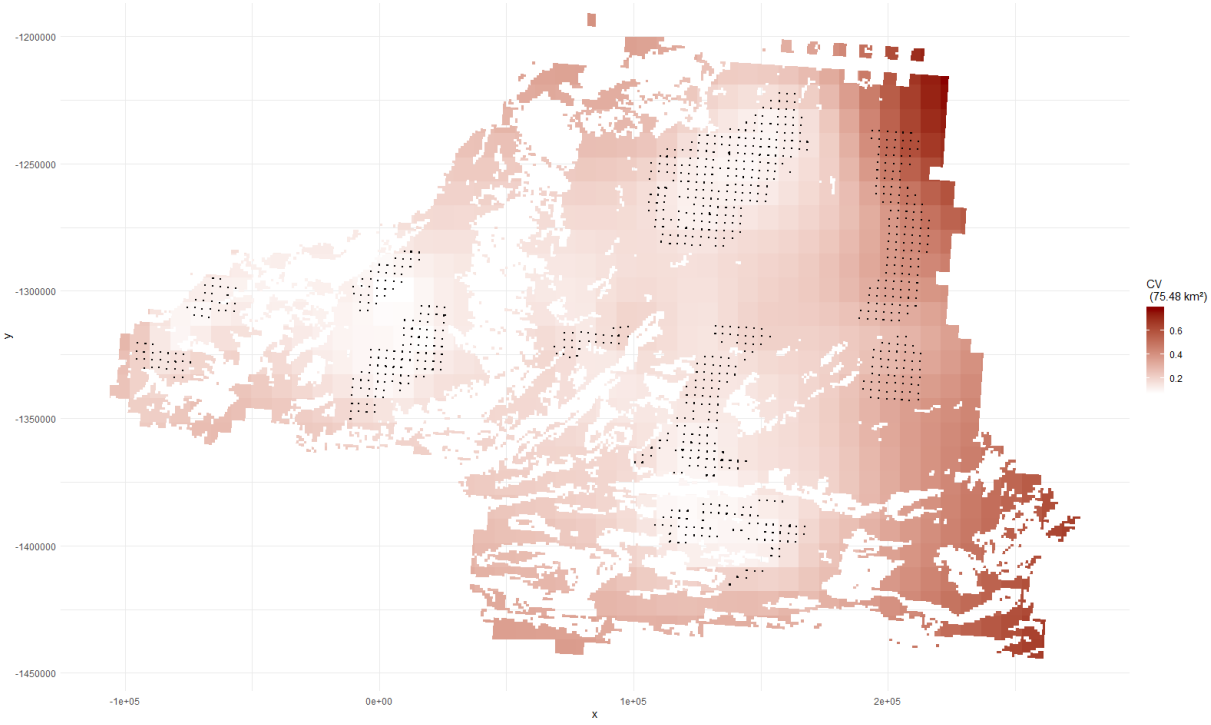

Figure A9: Spatial variation of uncertainty associated with the predicted abundance of houbara per pixel of 75km². projected in an area of 38.268 km². excluding some areas identified as unsuitable for the houbara (see Fig.A2-2 in Appendix S2). Uncertainty is given in terms of coefficient of variation of abundance estimates. Black dots represent the counting points.

Appendix S10: Annual density surface modelling (dsm)

We computed dsm analyses per year. We obtained distribution and uncertainty maps from 2010 to 2018 (Fig A10-1 and Fig A10-2). The annual distribution maps showed the spatial and temporal variation of the abundance of houbaras in the ECWP intervention area. Abundance is given in terms of absolute density by pixel of 75km². totaling a 38.268 km² of prediction area after the mask exclusion (Fig. A2-2). Uncertainty is given in terms of coefficient of variation of abundance estimates. Black points represent the counting points.

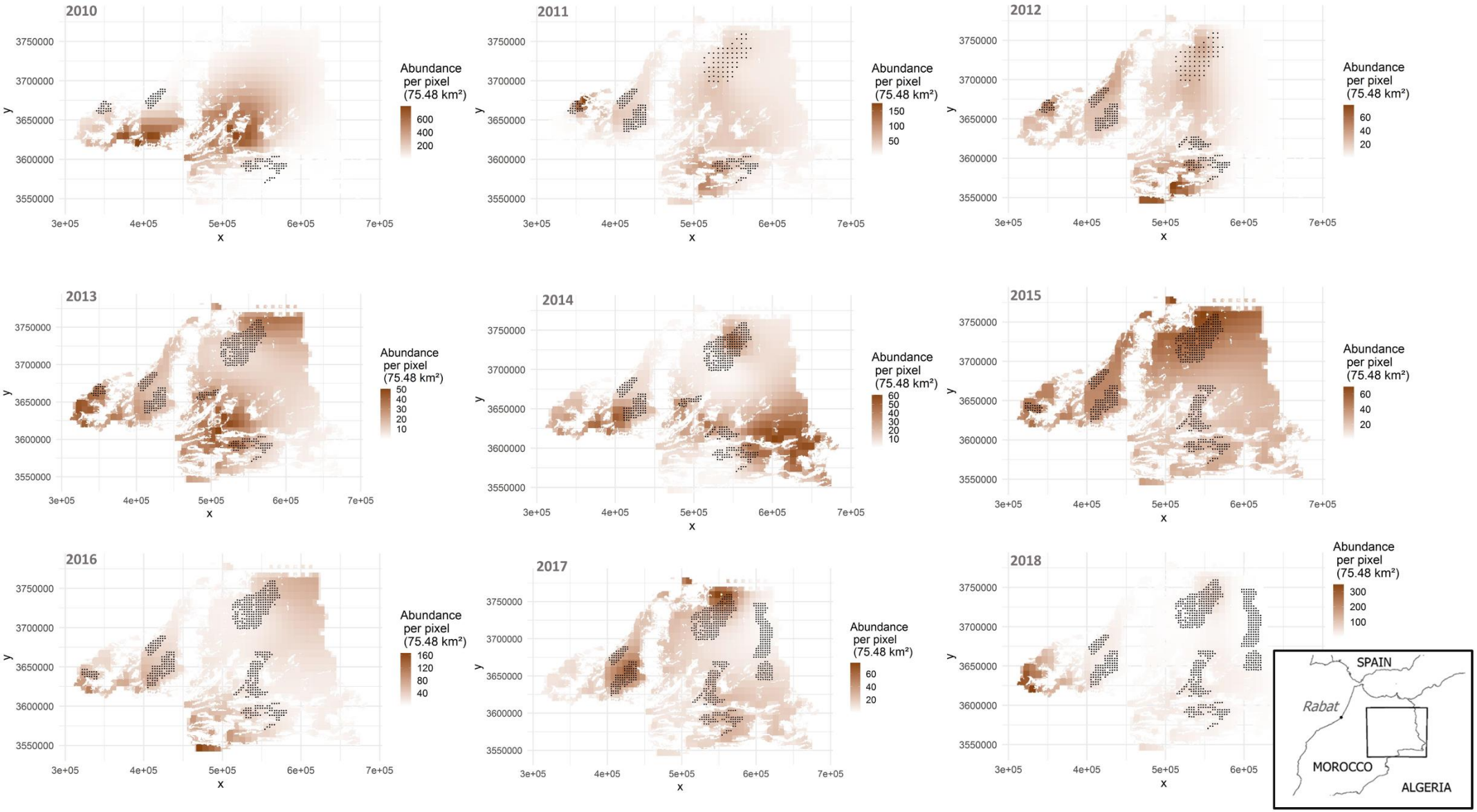

Figure A10-1: Spatial and temporal distribution maps of houbara abundance from 2010 to 2018. Number of individual per pixel of 75 km². Black dots represent the counting points.

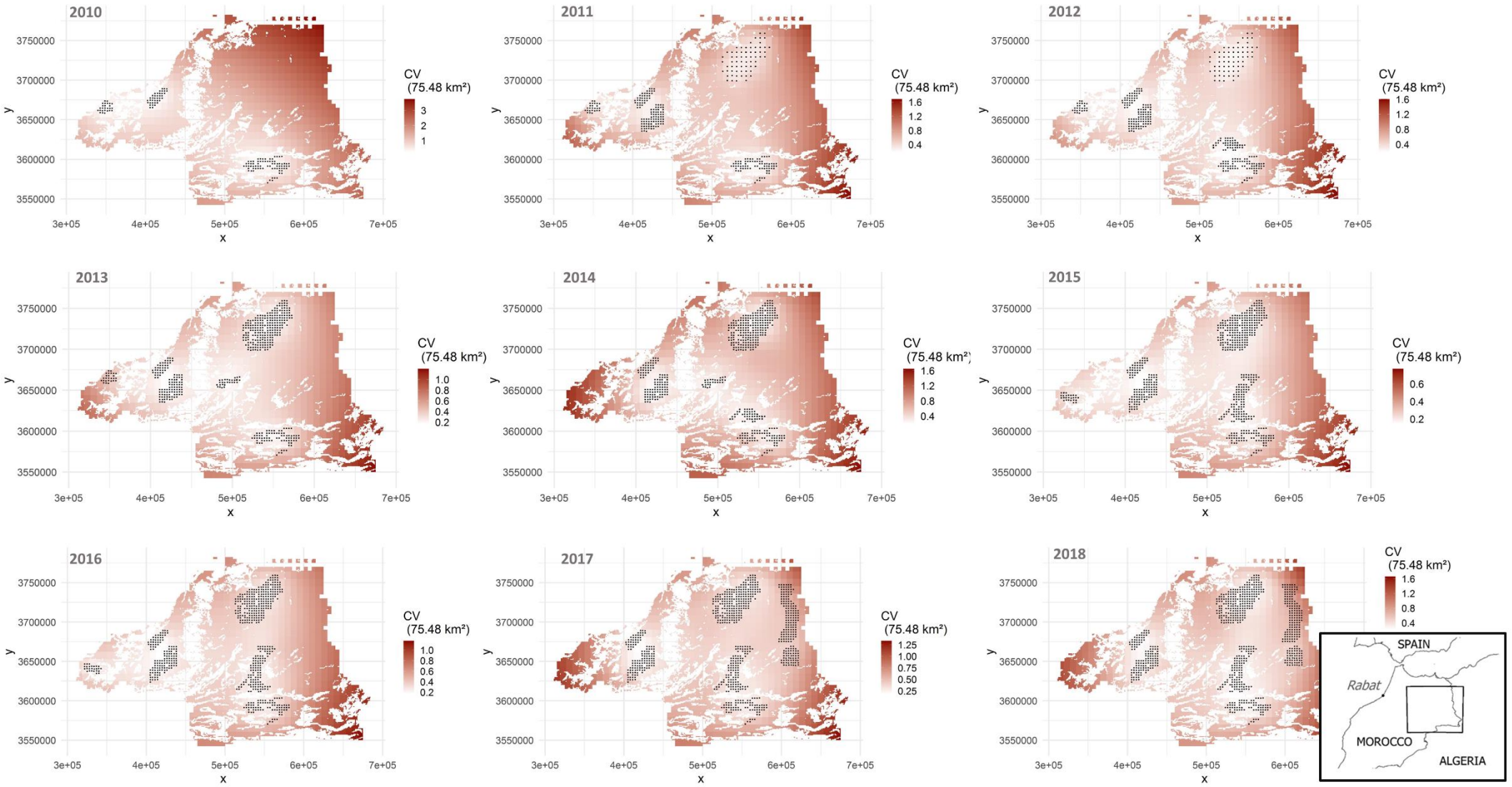

Figure A10-2: Spatial and temporal variation of uncertainty associated with the predicted abundance of houbaras from 2010 to 2018. Uncertainty was projected in an area of 38.268 km². excluding some areas identified as unsuitable for the houbara (see Fig. A2-2 in Appendix B). Uncertainty is given in terms of coefficient of variation of abundance estimates. Black dots represent the counting points.

Appendix S11: Correlation assessment and univariate models

To assess the correlation between the covariates used in the model. we tested the strength of the relationship between all the variables in the model by testing them in pairs. Using a correlation matrix (corrplot package; Wei *et al.*. 2017). we represented the correlation coefficients between variables. Positive correlations are represented on a blue scale while negative correlations are represented on a red scale.

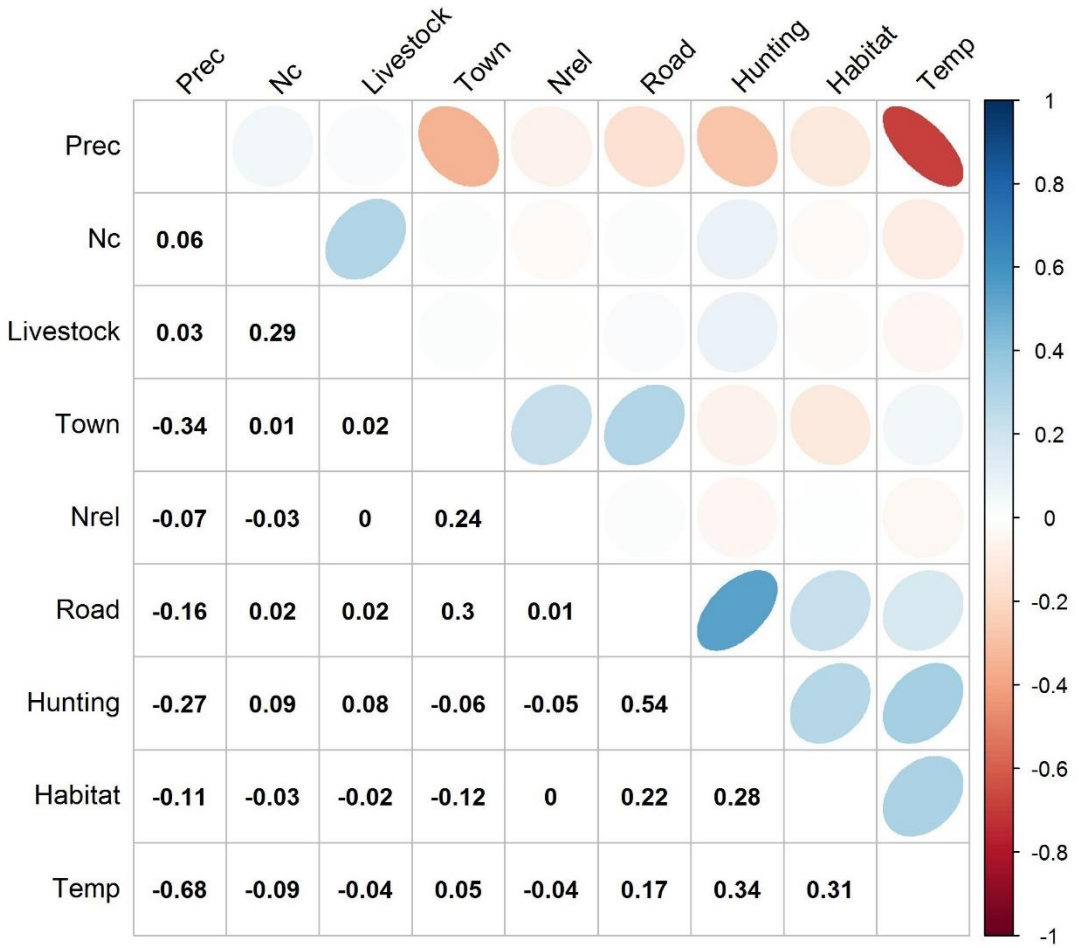

Figure A11: Assessment of correlations of covariates using a correlation matrix. Positive correlations are shown in blue. negative correlations in red. The intensity of the color and the size of the circle are proportional to the correlation coefficients (r).

This analysis showed negative correlations (r > -0.5) between the average temperature (Temp) and the mean precipitation (Precp) at a site. between the year (Year) and the anomaly of precipitation (Panom ; r=-0.54). and also between the anomaly of precipitation (Panom) and the anomaly of temperature (Tanom ; r=-0.5). Positive correlation (r > 0.5) was detected between the distance to the road (Road) and the management of the zone (Hunting) and also between the year (Year) and the anomaly of temperature (Tanom ; r=0.55).

In addition to correlation analyses. univariate responses of abundance to each covariate were tested separately using the same models as the main model (zero inflated) adding the Year as random variable. In Table A11. all the univariate models are compiled and ranked by AIC value. The univariate response of abundance to the type of management (Mod_Hunting). the number of livestock (Mod_Livestock) and to the number of releases (Mod_Nrel) showed a significantly positive relationship with abundance as in the multivariate model/selected full model. The univariate response of abundance to the temperature (Mod_Temp) showed a significantly negative relationship with abundance as in the multivariate model/selected full model. Some covariates showed a significant abundance response. not present in multivariate models: Mod_Town. Mod_Tanom and Mod_Road all had a significantly positive effect on abundance.

Table A11: Univariate models with each covariate tested against abundance (Nc). Models are ranked by AIC values. CI = Confidence Interval. Std.Error = Standard error.

		Estimate	CI (2.5%)	CI (97.5%)	Std.Error	P value	Significativity	AIC
Mod_Hunting	Hunting	0.39	0.32	0.46	0.04	<10e-3	***	40991
Mod_Livestock	Livestock	0.07	0.05	0.09	0.01	<10e-3	***	41065
Mod_Year	Year2011	-0.13	-0.28	0.02	0.08	0.002	.	41085
	Year2012	-0.62	-0.76	-0.48	0.07	<10e-3	***	
	Year2013	-0.75	-0.90	-0.61	0.08	<10e-3	***	
	Year2014	-0.50	-0.65	-0.35	0.08	<10e-3	***	
	Year2015	-0.29	-0.44	-0.14	0.08	<10e-3	***	
	Year2016	-0.39	-0.54	-0.24	0.08	<10e-3	***	
	Year2017	-0.28	-0.44	-0.12	0.08	<10e-3	***	
	Year2018	-0.77	-0.98	-0.56	0.11	<10e-3	***	
Mod_Town	Town	0.08	0.04	0.11	0.02	<10e-3	***	41088
Mod_Tanom	T_{anom}	0.11	0.06	0.17	0.03	<10e-3	***	41095
Mod_Nrel	N_{rel}	0.08	0.04	0.13	0.02	<10e-3	***	41097
Mod_Temp	Temp	-0.05	-0.08	-0.02	0.01	<10e-3	***	41098
Mod_Road	Road	0.05	0.02	0.08	0.02	0.001	**	41100
Mod_Panom	P_{anom}	-0.03	-0.07	0.02	0.02	0.293	NS	41109
Mod_Habitat	Hab_{mosaic}	-1.77	-3.59	0.05	0.93	0.057	.	41110
	Hab_{vege}	-0.02	-0.10	0.06	0.04	0.614	NS	
Mod_Prec	Prec	-0.01	-0.04	0.03	0.02	0.754	NS	41110

References in Supporting Information

Brooks ME. Kristensen KK. van Benthem KJ. Magnusson A. Berg CW. Nielsen A. Skaug HJ. Machler M. Bolker BM.. 2017. Modeling zero-inflated count data with glmmTMB. bioRxiv.

Hovmöller. E.. 1949. The Trough-and-Ridge diagram. Tellus 1. 62–66. https://doi.org/10.1111/j.2153-3490.1949.tb01260.x

Miller. D.L.. Burt. M.L.. Rexstad. E.A.. Thomas. L.. 2013. Spatial models for distance sampling data: recent developments and future directions. Methods Ecol. Evol. 4. 1001–1010. https://doi.org/10.1111/2041-210X.12105

Miller. D. L.. Rexstad. E.. Burt. L.. Bravington. M. V.. Hedley. S.. & Model. A.. 2020. Package "dsm".

Wei. T.. Simko. V.. Levy. M.. Xie. Y.. Jin. Y.. & Zemla. J.. 2017. Package 'corrplot'. Statistician. 56(316). e24.

Zuur. A. F.. Ieno. E. N.. Walker. N. J.. Saveliev. A. A.. & Smith. G. M.. 2009. Zero-truncated and zero-inflated models for count data. In Mixed effects models and extensions in ecology with R (pp. 261-293). Springer. New York. NY.